

Interior noise, Sound Pressure level, Statistical Energy Analysis, aircraft

A Statistical Energy Analysis (SEA) model of a fuselage section for the prediction of the internal Sound Pressure Level (SPL) at cruise flight conditions

Giuseppe Petrone, Giacomo Melillo, Aurelio Laudiero and Sergio De Rosa

Department of Industrial Engineering - Aerospace division, University of Naples Federico II, via Claudio 21, 80125, Napoli

Abstract

Nowadays, one of the priorities of the aircraft companies is to improve the passenger's comfort aboard the aircraft providing low noise level during the flight. The methods actually used for the evaluation of the noise level are various, the SEA is an example of these, which is able to obtain a high reliability on the results at increasing frequencies.

The goal of the present research is establish a numerical model to evaluate the Sound Pressure Level in the aircraft fuselage section at different stations and locations inside the cabin. Different configurations have been considered for the analysis: from the "naked" cabin up to "full furnished" with seats, stowage bins, etcetera. These results have been essential to understand which is the contribute of the aircraft interiors (seats, storage bins) on noise insulation. Furthermore the Power Inputs evaluation has been determined to see the contribution of each considered aeronautic component on the acoustic insulation and a final investigation by using a different type of window with the addition of a transparent viscoelastic damping material has been performed.

*Giuseppe Petrone
Email address: giuseppe.petrone@unina.it (Giuseppe Petrone, Giacomo Melillo, Aurelio Laudiero and Sergio De Rosa)

1. Introduction

Vibro-acoustic analysis is a necessary step for the virtual design of aerospace structures. In order to reduce the design costs and to maximize the acoustic performance of aerospace structures, a robust and mature prediction of interior noise levels is required.

Interior noise is an essential topic to be considered in the design and operation of all aerospace flight vehicles. Noise is due to the combination of different sources such as: powerful propulsion systems, high-speed aerodynamic flow over vehicle surfaces and operation of on-board systems (air conditioners, pressurization system) [[6, 7]].

High noise levels can be a negative aspect in the flight experience that can lead to problems such as passenger discomfort, interference with communication, crew fatigue, or malfunction of sensitive electronic equipment. They can produce temporary or permanent hearing loss, or cause other physiological symptoms, such as auditory pain, headaches, discomfort, strain in the vocal cords, or fatigue.

Noise is defined as undesirable sound. Excessive noise can result in psychological effects, such as irritability, inability to concentrate, decrease in productivity, annoyance, errors in judgment, and distraction [[1, 2]]. A noisy environment also can result in the inability to sleep or sleep well. Elevated noise levels can affect the ability to communicate, understand what is being said, hear what is going on in the environment, degrade crew performance and operations, and create habitability concerns. Superfluous noise emissions also can create the inability to hear alarms or other important auditory cues, such as the sound of an equipment malfunction [[5]].

In general, the noise level should be low enough to provide a feeling of comfort, avoiding in the noise spectrum excessive low-frequency "booming" or high-frequency "hissing".

The physics of noise transmission changes within a wide frequency regime, and in order to evaluate noise levels and vibration transfer paths in the whole

frequency range, there are various methods to consider [[8, 10]], because none of them has shown a complete reliability, but can be only used in a limited frequency region. According to wavelength there are two basic approaches: deterministic and statistical. In the low frequency range the behavior of a structure is deterministic and the basic tools applied for the analysis of vibration problems is finite element analysis (FEA) on the numerical side and experimental modal analysis (EMA) on the testing side [[11]].

Model validation of finite element models for the low frequency range is mainly based on the correlation of eigenvalues and eigenvectors from experiments and simulations. Modal analysis based on finite element has a long history in application to dynamic problem on engineering structure system, but this kind of method can be only used to analyze the low modal order which can be clearly identified.

In the high frequency range, instead, the behavior of a structure is stochastic which means that the statistics of the system have to be taken in consideration.

The use of the energy-based approaches in the aeronautical industry field becomes more appropriate to describe the propagation of vibrational energy through the structure in the mid to high frequency range. Foremost among them is the Statistical Energy Analysis (SEA) [[13]], which can be used both as theoretical and experimental technique. It provides a framework for predicting the dynamic response and analyzing the vibro-acoustic transfer paths of "weakly coupled" and complex structural-acoustic systems. Engineering applications of the SEA in built-up structures normally involve the analysis of all relevant transmission paths, and require a description of the power flow in a network of connected subsystems through the Coupling Loss Factor (CLF) [[14, 8]]. SEA is generally used for the prediction of interior noise of aircrafts and automobiles. There are a large number of studies in the industry for reducing the noise in aircraft and automobiles [[3, 4]]. Especially in the aircraft industry, there exist strict noise regulations leading the companies to improve their design in terms of acoustic insulation.

In this paper, a fuselage section model of a turboprop aircraft is defined

based on SEA approach. The numerical model is provided by the use of the commercial software VA One, within the SEA module. An example of a SEA model using the software VA One can be seen in [[15]]. The aim is to establish
65 a numerical model to evaluate the Sound Pressure Level in the aircraft fuselage section at different stations and location inside the cabin. Different configurations have been considered for the analysis: from the "naked" cabin up to "full furnished" with seats, stowage bins, etcetera. Moreover the Power Inputs evaluation has been determined to see the contribution of each considered aeronautic
70 component on the acoustic insulation and a final investigation by using a different type of window with the addition of a transparent viscoelastic damping material has been performed. All the data herein presented (interiors layout, geometry, materials,etc..) have been used in accordance and under authorization of Leonardo SPA.

75 **2. The basics of SEA theory**

The SEA method is able to evaluate the vibrational response at high frequencies. SEA is commonly used to predict interactions between reverberant sound enclosures and resonant structures [[16]].

The SEA model is commonly divided in a certain number of subsystems,
80 which are linked by junctions that provide the exchange of power flow [[8]]. These subsystems can be the wave types in a component. This leads to a considerable flexibility in identifying the subsystems when creating a SEA model. There are some guidelines for creating the subsystems [[9]]:

- For any particular band, each subsystem should contain a minimum number of modes whose natural frequency falls within the band. The "minimum number" can be taken as three to seven; however there is no significant definition for this.
85
- The energy should be equipartitioned between the modes of a subsystem, which means that no single mode or a small group of modes will dominate
90 the subsystems.

- The subsystems should be weakly coupled which means that if only one particular subsystem is subjected to excitation, the response of that subsystem will be significantly greater than that of any other subsystems.

The basic idea of SEA states that the power flow between two connected
 95 subsystems is related with the uncoupled resonant modes of the subsystems
 [[17]].

Under random loads, the subsystems are subject to external power inputs. Power may be dissipated due to damping mechanisms. The power always flows from the subsystem which has a higher modal energy, or energy per mode, to
 100 the one having lower modal energy. The subsystems consist of similar resonant modes within a structure or acoustic space. For example, for a flat plate the bending waves, shear waves and longitudinal waves can be treated as separate subsystems. Moreover, the subsystems can also be the physical components of a complex system. These subsystems are coupled via junctions through whom the
 105 energy is transferred. The power flow between the subsystems is proportional to the differences of the modal energies of the coupled system and the energy is dissipated within a subsystem related through loss factor. According to the basic concepts of SEA, the procedures are formulated by making the following assumptions:

- 110 1. The excitation spectrum is broadband and the excitation forces are statistically independent. There are no pure tones in the input spectra.
2. There is no energy generation or dissipation in the couplings between the subsystems.
3. The damping loss factor is the same for each mode within a subsystem
 115 and frequency band.
4. Modes within a subsystem do not interact except to share equipartitioned energy.

The power always flows from the subsystem which has a higher modal energy to the one having lower modal energy through dynamic equilibrium. These
 120 arguments are synthesized in the following equation:

$$P_{ij} = \omega(\eta_{ij}E_i - \eta_{ji}E_j) \quad (1)$$

where ω is the analysis band center frequency; η_{ij} and η_{ji} are the coupling loss factors when the power flows from subsystem i to subsystem j and from subsystem j to subsystem i , and E_i and E_j are the uncoupled total subsystem energies. SEA assumes that in narrow frequency bands, all modes have the same energy at steady-state. Here, an important reciprocity relationship for SEA must be introduced:

$$\eta_{ij}n_i = \eta_{ji}n_j \quad (2)$$

By using Eq. (1) and Eq. (2), the general SEA power flow equation can be represented as:

$$P_{ij} = \omega\eta_{ij}n_i \left(\frac{E_1}{n_1} - \frac{E_2}{n_2} \right) \quad (3)$$

The total energy in each element in a frequency band with a center frequency of ω can be found by the equation: In this equation, n_i represents the modal density of the element in the frequency band interested, and e_i represents the modal energy of the element. Moreover, the power dissipated within the system can be found by using the internal loss factor of the element, η_i , with the equation:

$$P_{i,diss} = \omega\eta_iE_i \quad (4)$$

By using Equation 3 and Equation 4, the power balance for subsystem i can be written as:

$$P_{i,in} = P_{i,diss} + P_{ij} \quad (5)$$

$$P_{i,in} = \omega\eta_i E_i + \omega\eta_{ij} n_i \left(\frac{E_1}{n_1} - \frac{E_2}{n_2} \right) \quad (6)$$

In most general form, for a complex system having more than two subsystems connected to each other, for example s subsystems, equation (6) can be written as:

$$P_{i,in} = \omega\eta_i E_i + \sum_{j=1}^s \omega\eta_{ij} n_i \left(\frac{E_i}{n_i} - \frac{E_j}{n_j} \right) \quad (7)$$

140 To implement SEA for a system that is comprised of N subsystems, the power balance equations are expressed using the following generalized matrix solution ([17]) to determine the energy vector from:

$$\{P_{in}\} = \omega[L]\{E\} \quad (8)$$

where ω is the central frequency of a frequency band, E is the energy vector and P_{in} is input power vectors, $[L]$ is the loss factor matrix that includes the 145 damping loss factors and coupling loss factors, whose elements are given by:

$$L_{ij} = \begin{cases} -\eta_{ij} & i \neq j \\ \sum_{k=1}^N \eta_{ik}, & i = j \end{cases} \quad (9)$$

Here, the damping loss factor and coupling loss factor are determined by the characteristics of the subsystems themselves. According to equation (9), if the system parameters (loss factors η_i , coupling loss factors η_{ij} , modal densities n_i , power inputs and the analysis center frequency) are known, the energy 150 distribution of the subsystems can be found. In summary, the general procedure for SEA calculations is as follows:

1. Specify the frequency bands for the analysis;
2. define the subsystems;
3. calculate the subsystem properties, namely modal density, loss factor and
155 the coupling loss factor;
4. determine the external power input to each subsystem;
5. formulate the power balance equation, which is the equation (7);
6. solve the equation to obtain the average energy in each subsystem;
7. convert average subsystem energies into desired response quantities.

160 3. SEA modeling of a fuselage section

A fuselage section has been modeled using the software VA One, through the SEA module. This section is 7.2 m long and corresponds to the most loaded section because of the presence of the turboprop wing-mounted engines close to the fuselage, although in this study the tonal loads in the low frequency range
165 are neglected.

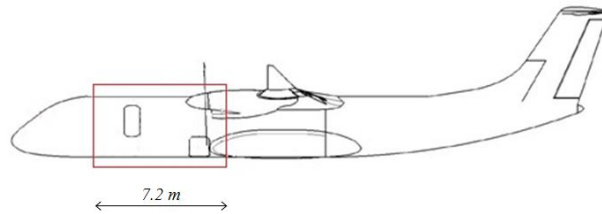


Figure 1: Side view of a turboprop aircraft

A side view of the SEA fuselage model is shown in Fig. 2, where it can be noted that the fuselage section has been divided in 6 subsections in order to distinguish the Sound Pressure Level (SPL) along the fuselage at 6 different stations, necessary to evaluate the noise level at various distances from the noise
170 source. The subsection I is the farthest from the turboprop engine source. The most loaded subsection is the VI, which is the closest to the engine.

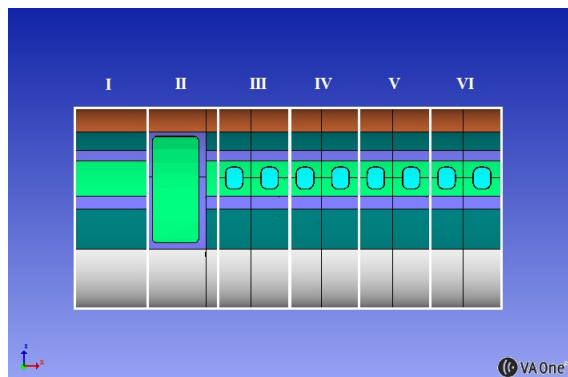


Figure 2: Side view of the SEA model. Fuselage section partitioning

A front view of the SEA fuselage model is shown in Fig. 3, where it can be noted the internal subdivision through the cavities. A cavity is a SEA subsystem defined in VA One with the physical property of an acoustic fluid. A fundamental property associated to a cavity is the damping coefficient, that can be defined as: damping loss factor, absorption from noise control treatment or average absorption.

The internal arrangement of the acoustic cavities is shown in Fig. 3. It can be noticed that the internal pattern is divided in 3 main zones, which are named as follow:

- Head cavity
- Leg cavity
- Corridor cavity

This kind of division of the SEA acoustic cavities is useful to understand how the SPL is distributed over a subsection. In particular, the attention has been focused on the "Head cavity", because the energy level measured in this cavity is correlated to the SPL perceived by the human ear.

The seating arrangement is shown in Fig. 4. It can be seen that there is a 3+2 seat layout, so it is not-symmetric. The seats have been modeled using a typical aeronautic seat foam, that both with the other absorbing materials,

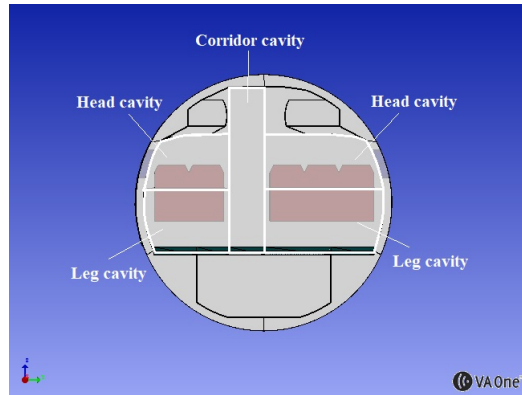


Figure 3: Internal arrangement of the SEA acoustic cavities over a subsection

provide an absorption of the vibrational energy inside the cabin, so the reduction of the noise level, when they are installed aboard.

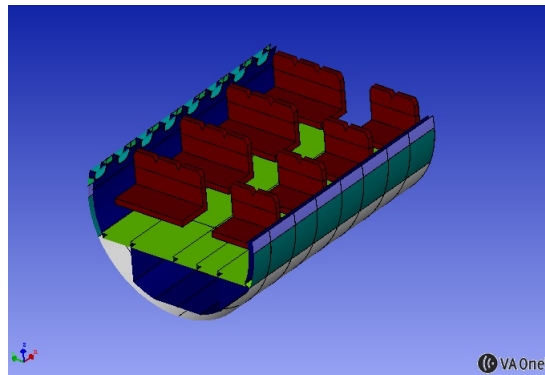


Figure 4: Seating layout arrangement

Finally the SEA model including the application of the external loads and the Semi Infinite Fluids (SIF) is reported in Fig.5. The fuselage section has
 195 been represented with 582 SEA plates and 126 acoustic cavities and the input power has been derived from a turbulent boundary layer (TBL) model.

The Turbulent Boundary Layer (TBL) has been calculated by the software [18], following two characteristics:

1. a band-limited RMS pressure spectrum, considering the Robertson semi-

200

empirical model ([19, 20]);

2. a narrowband Spatial Correlation Function between the pressure fluctuations at any two points on the loaded surface.

The parameters required for the TBL calculation are listed below:

- U_0 = free stream flow velocity
- 205 • X_0 = distance from the leading edge of the TBL to the center of the pressure load on the surface of the subsystem
- δ = Turbulent Boundary Layer Thickness (defined as the distance from the wall where the fluid velocity equals 99 percent of the free stream velocity)
- c_x, c_y = the spatial correlation coefficients of decay in the along-flow and cross-flow directions
- 210 • k_x, k_y = the projections onto the local axes of the convection wavenumber k_c

The root mean square spectrum due to TBL has a mean value of 105 dB.

- Furthermore, the Semi Infinite Fluid (SIF) represents an unbounded exterior
- 215 acoustic space. The acoustic waves radiated by a subsystem connected to a SIF are not reflected back on the subsystem.

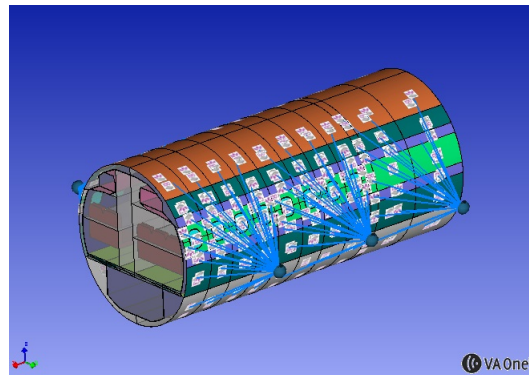


Figure 5: SEA model of a fuselage section including the application of external loads and SIF

3.1. Materials

A fuselage section is a complex structure made of several different materials, isotropic and orthotropics, and inside orthotropic different lay-ups according to the components. In view to have a clear view of the material distribution a list of the materials used for each structure modeled in the fuselage section is here listed and shown in Fig. 6:

- **Skin:** Composite panels made of carbon fibre reinforced epoxy resin having different lay-up and stacking sequence according to the component.
- **Trim panel:** Sandwich panels consisting of a thermoplastic foam core embedded between two skins made of fabric glass.
- **Floor:** Isotropic panel made of rigid foam covered by a carpet.
- **Seat:** Aluminium structure covered by a typical aeronautical seat foam.
- **Window:** A thick window layout composed of a tempered glass, airgap and plexiglass clamped between two aluminium frames.

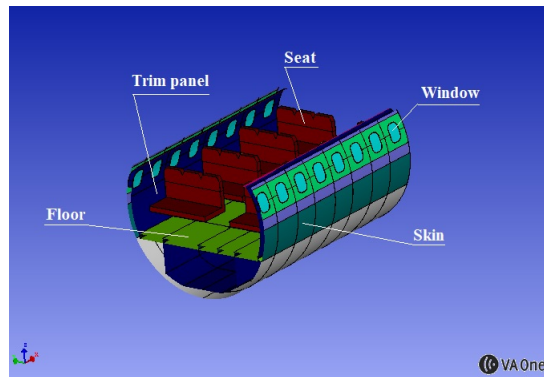


Figure 6: SEA model of a fuselage section

Furthermore, over the structural materials, in order to reduce the internal noise, in such case a soundproofing material is added to the structure. A typical fuselage is composed of a skin, stiffeners and frames, an insulation layer and an

interior wall. The absorption materials such as the fabric and the soft foam
 235 are usually used in the insulation layer to improve the sound insulation (Fig.
 7). One principal function of absorbent materials in-between two panels is to
 suppress acoustic resonances of the cavities that would otherwise strongly couple
 the two panels. Another principal function is to decouple the trim sheet (interior
 wall) from the vibration field induced in the outside structural shell by various
 240 acoustic and mechanical sources



Figure 7: Typical sidewall treatment of a large passenger transport aircraft

In this work a 10 cm thick of glass wool blanket has been used by means
 of the application of Noise Control Treatment (NCT). Absorption coefficient is
 reported in Fig. 8 while some characteristic properties are reported in Table 1.

Table 1: Properties of the *glass wool* blanket

Properties of the <i>glass wool</i> blanket	
Porosity	0.99
Tortuosity	1
Viscous characteristic lengths [m]	0.000192
Thermal characteristic lengths [m]	0.000384
Flow resistivity [Ns/m^4]	9000
Density [Kg/m^3]	16

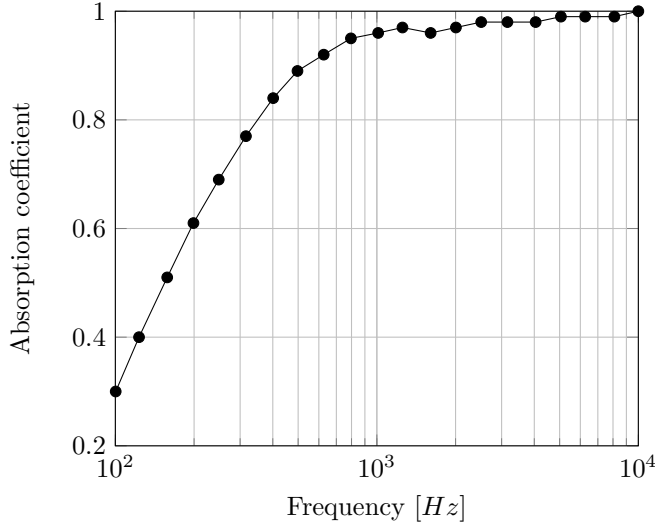


Figure 8: Absorption coefficient of a 10 cm width glass wool layer.

3.2. Fuselage section configurations

245 The elements of importance to interior noise include the fuselage structure and the acoustic treatments in the cabin. A calculation procedure that can rigorously handle these elements and their interactions is not yet available. Therefore approximate methods are required, such as the bottom-up approach where the Sound Pressure Level is calculated step by step starting from the basic primary structure (*naked*) up to the fuselage including the interiors and the secondary structures (*fully furnished*).
 250

The analyzed configurations are:

Configuration A: the fuselage section has been modeled considering the only primary structures, as can be seen in Fig. 9.

255 **Configuration B:** the model includes the primary and secondary structures, but no interiors have been installed. As can be seen in Fig. 10 the internal arrangement of the SEA cavities remain the same of that in conf. A, but the difference is the presence of the air gap cavities between the skin panels and the internal panels.

260 **Configuration C:** the arrangement of the model is the same of the conf.

B, but in this case the NCT has been added between the primary and secondary structures.

Configuration D: is a result of the conf. B including the interiors (seats, stowage bin) as we notice in Fig. 11.

265 *Configuration E*: is a result of the conf. D including the presence of NCT.

4. Results

In the analysis has been considered the condition of cruising flight at an altitude of 6000m with a flight speed of 177.5 m/s. The values of cinematic viscosity, density and speed of sound at 6000m of altitude have been given to the fluid. These values have partially characterized the TBL and SIF parameters applied to each panel of the model. For the internal cavities, the parameters of the fluid correspond to those at sea level. In each section of the fuselage X_0 was given considering a value starting from 3m in section I up to 10m in the last one, section VI, as shown in Fig. 13.

275 The first results it has been represented is the SPL over the interior cavities of the fuselage. The SPL has been plotted in dBA to better represent the human ear perception of noise.

As it is well known, the accuracy of the SEA analysis increases with the raise of the Modal Overlap Factor (MOF). Generally, a MOF higher than 1 provides a good reliability of the results. This happens because, at low frequency, where there are few modes, SEA results are poor and exact results present a high sensitivity to the position of the excitation point. Increasing frequency, modal overlap factors and modes number increase; then SEA results are better and the sensitivity to the position of excitation decreases. The explanation is that increasing the damping smooths the frequency response functions of the systems, making them less sensitive to variations in structural details. There are empirical rules that say that the statistical variances are acceptably small if the modal overlap factors of the subsystems are greater than a certain value (1.0 is a commonly quoted number). As shown in Fig. 14 the MOF associated

290 with the SEA cavities of the model is higher than 1 starting from the frequency
1000 Hz. For this reason, the frequency range that has been adopted in the
analysis is 1000-10000 Hz.

In Fig. 21 is shown the SPL of the Head Cavities present in the fuselage
section. The Figg. 15,17,19 are referred to the cavities which correspond to the
295 three-seat layout, while the Figg. 16,18,20 are referred to the cavities which
correspond to the two-seat layout. These results are related to the region of
space occupied by passengers' ears.

As can be seen from the SPL curves, the behaviour is decreasing as the
frequency increases, for all the cases and the cavities analysed. This is partly
300 due to the trend of the TBL pressure spectrum, as can be seen in Fig. ??, that
from 1000 Hz has shown a decreasing behaviour. The other factor contributing
to this SPL trend is the Damping Loss Factor (DLF) of the materials and the
absorption coefficients of the NCT and of the foam present on the seats.

It is possible to see that for all the cavities, the maximum SPL is about
305 91 dBA for the *configuration A* at 1000 Hz. Considering the *configuration A*,
the SPL variates between the 91 dBA at 100 Hz and the 70 dBA at 10000 Hz.
Looking at the results shown for the SPL of the *configuration B*, where it has
been considered the primary structure plus the trim panels, the SPL variates
from 91 dBA at 1000 Hz to 52 dBA at 10000 Hz, that is almost 20 dBA lower
310 than the previous case. For the *configuration C* it is possible to see the effect
of the NCT on the sound insulation. In fact, the SPL curve in this case is
constantly about 4 dBA lower than that of the *configuration B* this means also
lower value for the OASPL. The SPL curve of the *configuration D* is essential
to understand the effect of the interiors on noise reduction. It is interesting to
315 see that the SPL values of the *Configuration D* and *E* are much lower than the
other configuration and also the effect of the seat layout provide differences not
negligible. The SPL curve associated to the cavities over a three-seat layout is
lower 3 dBA than than the SPL curve related to the cavities over the two-seat
layout.

320 In order to better represent the next results, an enumeration of the SEA

cavities has been specified as shown in Fig. 22, where it has been considered all the Head Cavities and Corridor Cavities.

In Fig. 23 is shown the OASPL (dBA) over different cavities along the fuselage, comparing the results for all the configurations.

325 As it was expected, the worst configuration is the *configuration A*, since the OASPL reaches values of 96 dBA for almost all the cavities considered.

In *configuration B* where it has been considered also the trim panel, the OASPL is about 2 dBA lower than that in *Configuration A*.

330 When adding a layer of 10 cm of glass wool, as defined in the *Configuration C*, it is possible to notice an improvement of 3 dBA respect to the *configuration B*. In this case the average OASPL is about 90 dBA.

From this graph it is clear that the OASPL of the first three configurations described is rather constant. This happens because of the non-presence of the seat layout, which has been defined made of a damping material, that provide
335 a reduction of the acoustic vibrations inside the SEA cavities.

Looking at the OASPL results of the *configuration D*, it is possible to observe the positive effect granted by the interiors on the noise level. In this case the average OASPL is nearly 84 dBA, about 9 dBA lower than the analogous case without the interiors and without the NCT, or rather, the *configuration B*.
340 Furthermore, the OASPL is not constant over the fuselage, while it changes if it is considered the three-seat layout or the two-seat layout. In the cavities defined over the three-seat layout, the result is even 4 dBA lower than the results observed in the cavities with a two-seat layout. This happens as a result of the less presence of foam material, that produce a smaller damping.

345 The *configuration E* is the one that has reported the minor OASPL, with an average value of 81 dBA. In this case too, it is notable the difference in OASPL over the two-seat layouts.

In consequence of these results, it is possible to assert that the addition of damping materials is fundamental for the reduction of the internal noise inside
350 the fuselage cabin. In effect, in order to keep the same OASPL over the different seat-layouts, a solution could be increasing the thickness of the glass wool layer

along the two-seat layout side, providing a higher damping of the vibrational energy inside the cabin, paying attention to weight gain.

In Fig. 24 is shown the contour plot of the OASPL, considering the only 355 *configuration E*, because it results to be the adopted configuration because of its lowest OASPL. Thanks to this colored representation it is possible to see the difference in noise level for different passenger positions and along the fuselage. The information of main interest is the difference between the OASPL over the two sides of the fuselage. The assessed OASPL variates from 79 dBA to 83 dBA 360 when moving from the two-seat layout to the three-seat layout.

Before discussing about the next results, or rather the Power Inputs, it has been represented in Fig. 25 one of the section of the fuselage model, renaming the needed SEA subsystems, in order to make the representation of the results more comprehensible.

365 The Power Inputs graphs consist of the following curves for each enabled wavefield in the selected subsystems. This field is referred to as the receiver:

- Total power to the receiver from all sources.
- Every power applied to the receiver.
- Every wavefield of every connected SEA subsystem that contributes power 370 to the receiver in any band.

The subsystem, which Power Inputs are referred to, is the Head Cavity of the section III over the two-seat layout. It has been chosen this specific cavity because it results the cavity with the highest OASPL for the configuration that has shown the lowest noise levels, or the *configuration E*.

375 The results are shown in Fig. 30, considering the configurations B, C, D and E.

It is possible to see that the main sources for this cavity that contribute to a high SPL are those closer to the windows. For each configuration considered, the highest source in the range of frequency 1000-2000 Hz is provided by the

380 external windows, while afterwards the SEA subsystems that provide the highest energy source are those around the windows.

Furthermore, it can be seen that starting from 2000 Hz, the Power Inputs related to the configurations without the presence of NCT, are quite higher than those of the configurations with the NCT. This happens because the NCT
385 provide a damping of the vibrations that come from the SEA subsystems, that are in turn excited by the external loads.

The Power Inputs evaluation is fundamental to understand which are the subsystems that involve the highest source of energy inside the cabin. Thanks to this, a correction on the subsystems' parameters, such as thickness, materials
390 and geometry can be considered to improve the sound insulation properties. In this case a good solution to reduce the energy transmitted inside the cabin could be increasing the thickness of the panels around the windows, or maybe, changing materials which they are made of.

In the current research, since the results obtained from the power inputs,
395 it has been considered a new window layout, having the same mass of the previously adopted, in order to reduce the structure-borne and the air-borne noise transmitted into the interior. For the new window layout, the 3 mm thick layer of tempered glass has been substituted with two layers of tempered glass (1.7 mm and 1 mm) with transparent viscoelastic damping material sandwiched
400 between the layers, which has a thickness of 0.6 mm, as shown in Fig. 31. The used viscoelastic damping material is the Solutia Saflex, which has a density of $1068 \frac{kg}{m^3}$, the Poisson's ratio is 0.499, while the shear modulus and the damping coefficient varies with frequency and are shown in Figg. 32, 33.

In Fig. 37 is shown the comparison of the SPL in the aircraft interior between
405 the *Configuration E* and the *Configuration E + Viscoelastic interlayer* in the frequency range 1000-10000 Hz. In this case it has been considered only the Head Cavity of the section III because it appears to be the most critical in terms of internal SPL. It is possible to see that the improvement provided by the presence of the viscoelastic interlayer are quite evident at 1000 Hz, where
410 the SPL is 4 dBA lower than the *Configuration E* case, while starting from 1500

Hz the improvement is constantly equal to 1 dBA.

The comparison of the OASPL between the *Configuration E* and the *Configuration E + Viscoelastic interlayer*, along the cavity numbered as in Fig. 22, is shown in Fig. 38. It is possible to notice that the presence of the Saflex interlayer
415 ensure an OASPL 2 dBA lower than the one evaluated for the *Configuration E*,
in both the cavities over the two-seat and three-seat layout.

5. Conclusion

In this research, different results on the vibrational energy related to the internal aircraft cabin have been presented. Five configurations have been presented, starting from the single primary structure to the definition of the complete fuselage section, including trim panels, interiors and passive noise control
420 materials. The OASPL along the fuselage has been evaluated, considering the TBL load and the load due to the turboprop engine, in a range of frequency from 100 Hz to 10000 Hz. The difference between the *Configuration A* and the
425 *Configuration E* in terms of OASPL along the fuselage is even of 18 dBA. The results have shown that damping materials used for the passive control (Glass wool) and for the seat configuration (typical aeronautical seat foam) have greatly contribute on noise reduction. The application of a 10 cm thick layer of glass wool is able to reduce the SPL of about 4 dBA. The definition of interiors inside
430 the cabin (seats, storage bins) produce a strong noise insulation. The difference on SPL are strongly appreciable even moving from a two-seat layout to a three-seat layout.

Furthermore, a new window layout has been defined, sandwiching a viscoelastic damping layer between two tempered glass layers. This new layout
435 has provided an significant reduction of the internal SPL, that is about 2 dBA for the cavities close to the windows. These results have shown that the use of viscoelastic layers for a new window layout can be a valid alternative to the conventional windows.

However, a noise control plan strongly is recommended, and it should be

440 updated throughout the design, the manufacturing stages, and all flight phases
of the space vehicle. The noise control plan, in combination with monitoring
and oversight of the design, development, and verification efforts, is essential to
achieve full compliance with the defined acoustic requirements.

6. Acknowledgments

445 This project has received funding from the Clean Sky 2 Joint Undertaking
under the European Union's Horizon 2020 research and innovation programme
under grant agreement NCS2-AIR-GAM-2014-2015-01. The studies performed
on the new window layout, consisting of a viscoelastic damping layer between
two tempered glass layers, are outside the activities of the project.

450 References

- [1] Muhm , J. Michael and Rock , Paul B. and McMullin , Dianne L. and
Jones , Stephen P. and Lu , I.L. and Eilers , Kyle D. and Space , David R.
and McMullen , Aleksandra]Effect of Aircraft-Cabin Altitude on Passenger
Discomfort, The New England Journal of Medicine, 357:18-27.
- 455 [2] Ahmadpour, N., Robert, J.M. and Lindgaard, G., Aircraft passenger com-
fort experience: Underlying factors and differentiation from discomfort,
Applied Ergonomics,52, 301-308, 2016
- [3] Koukounian, V.N., Mechefske, C.K. (2018), Computational modelling and
experimental verification of the vibroacoustic behavior of aircraft fuselage
460 sections, Applied Acoustics, 132, 8 - 18.
- [4] De Langhe K., Peiffer, A., Boeykens, R., Moser, C. (2016), Sound Trans-
mission Loss predictions of aircraft panels: an update on recent technology
evolutions, Proceedings of INTERNOISE 2016 21-24 August 2016,Ham-
burg, Germany.
- 465 [5] Allen C.S. (2017), Internal Acoustics of the ISS and other spacecraft, Pro-
ceedings of ACOUSTICS 2017 19-22 November 2017,Perth, Australia.

- [6] Filippone A.(2014), Aircraft noise prediction, Progress in Aerospace Sciences, 68, 27–63.
- [7] Wilby, J.F.(1996) Aircraft interior noise, Volume 2, Journal of Sound and
470 Vibration, 190(3), 545-564.
- [8] Bouhadj, M., von Estorff, O., Peiffer A (2017), An approach for the assessment of the statistical aspects of the SEA coupling loss factors and the vibrational energy transmission in complex aircraft structures: Experimental investigation and methods benchmark, Journal of Sound and Vibration,
475 403, 152 – 172.
- [9] ESDU (1999), An Introduction to Statistical Energy Analysis, Item 99009.
- [10] Yan, Y., Li, P., Lin H. (2012), Analysis and experimental validation of the middle-frequency vibro-acoustic coupling property for aircraft structural model based on the wave coupling hybrid FE-SEA method, Proceedings
480 of 2012 International Conference on Mechanical Engineering and Material Science.
- [11] Viken N.K., Mechefske, C.K. (2018),Computational modelling and experimental verification of the vibro-acoustic behavior of aircraft fuselage sections, Applied Acoustics 132, 8 – 18.
- 485 [12] Wilby, J. F.(1982), Propeller Aircraft Interior Noise. Propeller Performance and Noise, Volume 2, VKI-LS-1982-08-VOL-2, Von Karman Institute for Fluid Dynamics.
- [13] Lyon, R.H., DeJong, R.G. (1995), Theory and application of Statistical Energy Analysis, 2nd edition Butterworth-Heinemann, Boston.
- 490 [14] Culla, A., D’Ambrogio, W., Fregolent, A., Milana S. (2016), Vibroacoustic optimization using a statistical energy analysis model, Journal of Sound and Vibration 375, 102–114.

- [15] Zhang, J., Xiao, X., Sheng, X., Zhang, C., Wang, R., Jin, X. (2016), SEA and contribution analysis for interior noise of a high speed train, Applied Acoustics 112, 158–170.
- 495
- [16] Mohamed, Z., Wang, X. (2016), A deterministic and statistical energy analysis of tyre cavity resonance noise, Mechanical Systems and Signal Processing 70-71, 947-957.
- [17] Lyon, R.H. (1975), Statistical Energy Analysis of Dynamical Systems: Theory and Applications, The MIT Press.
- 500
- [18] VA One (2016), User’s guide.
- [19] Cockburn, J.A., Robertson J.E. (1974), Vibration Response of Spacecraft Shrouds to In-flight Fluctuating Pressures, Journal of Sound and Vibration, 33(4), 399-425.
- 505 [20] Miller, T.S., Gallman, J.M., Moeler, M.J. (2012), Review of turbulent boundary layer models for acoustic analysis, Journal of Aircraft, 49(6), 1739-1754.

[t]0.475

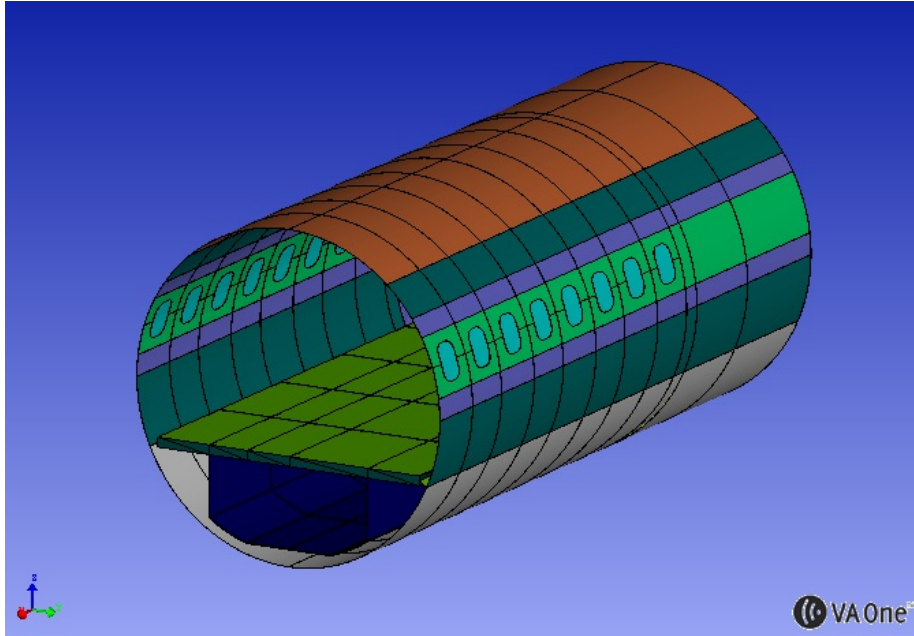


Figure 9: SEA model of a fuselage section. Configuration A

[t]0.475

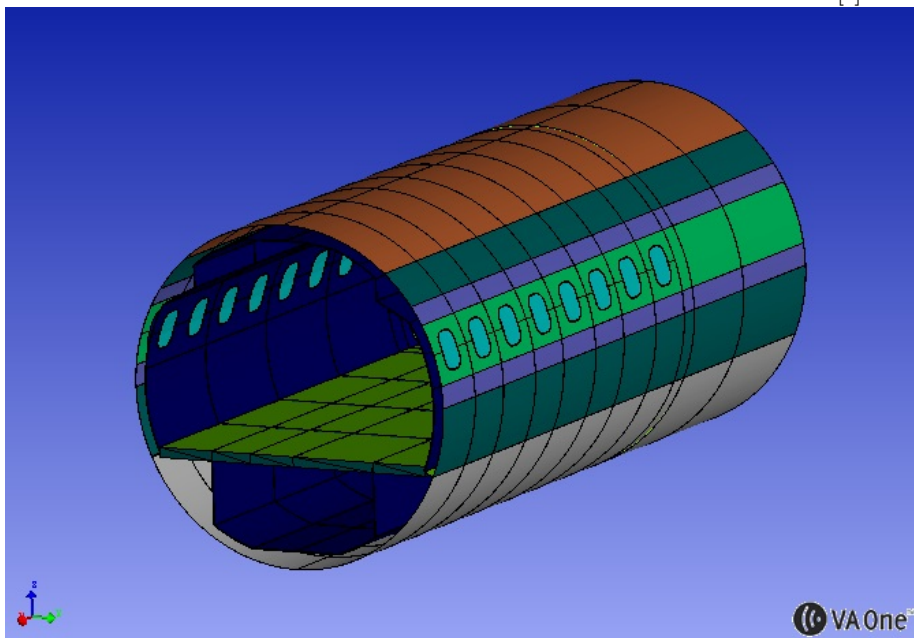
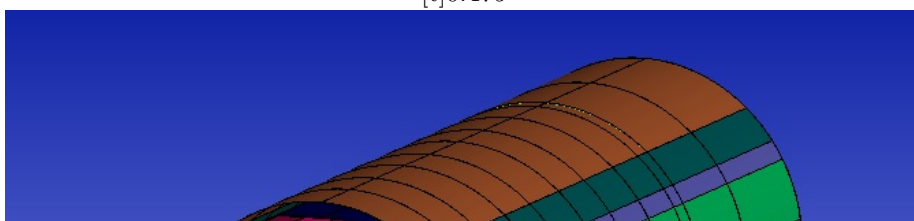


Figure 10: SEA model of a fuselage section. Configuration B

²⁵
[t]0.475



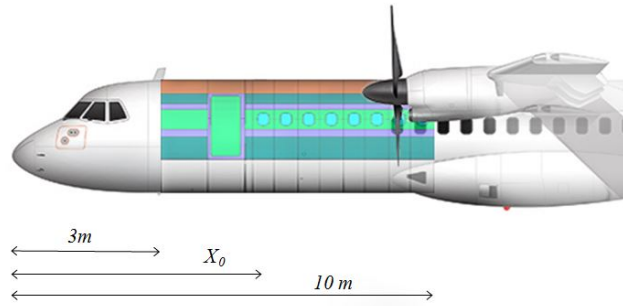


Figure 13: Description of the parameter X_0 used for the TBL calculation along the fuselage section

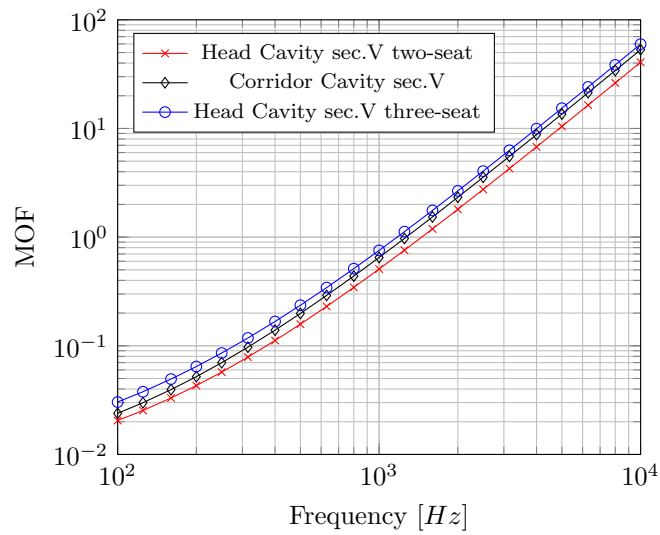
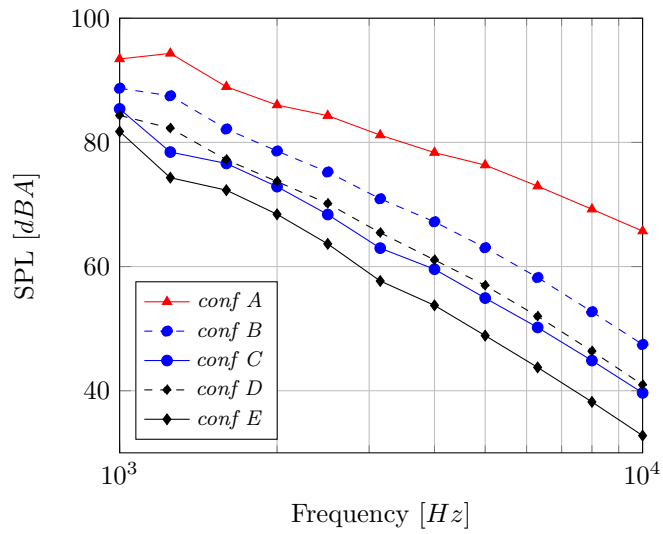
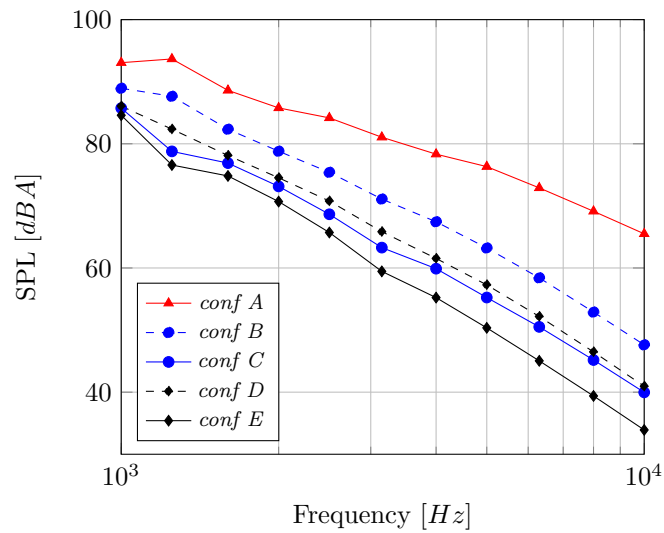


Figure 14: Modal Overlap Factor of different SEA cavities in the fuselage section. Frequency range: 100-10000 Hz



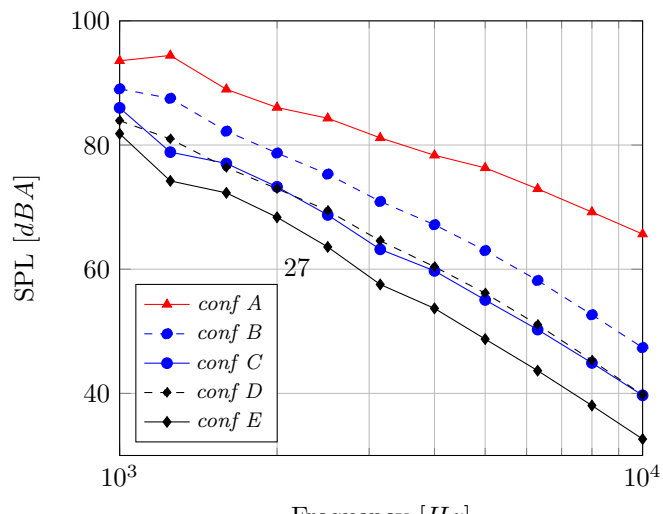
[t]0.48

Figure 15: Head cavity: Sec. III - three-seat layout side



[t]0.48

Figure 16: Head cavity: Sec. III - two-seat layout side



Frequency [Hz]

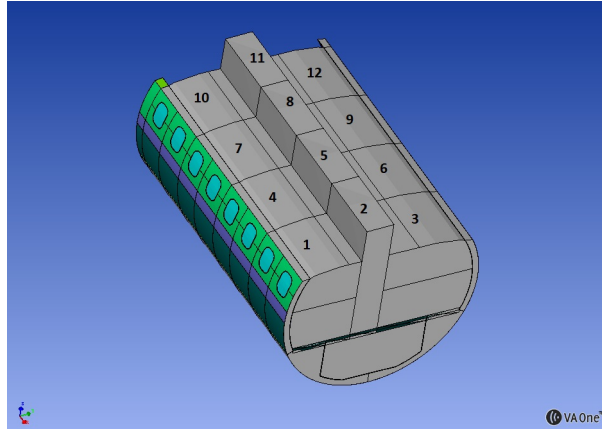


Figure 22: Internal enumeration of the SEA cavities along the fuselage section

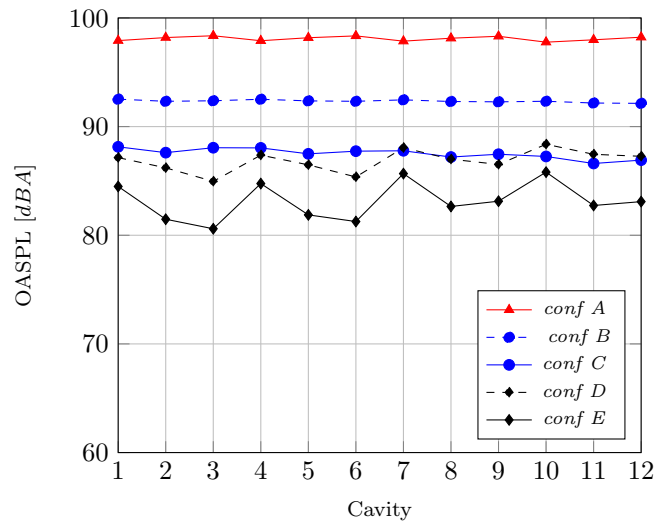


Figure 23: OASPL over the cavities present in the fuselage section. Comparison between the configurations analyzed

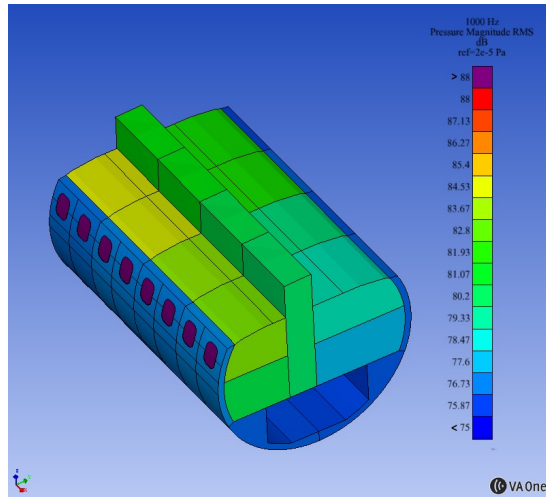


Figure 24: OASPL (dBA) inside the aircraft cabin of the *Configuration E*

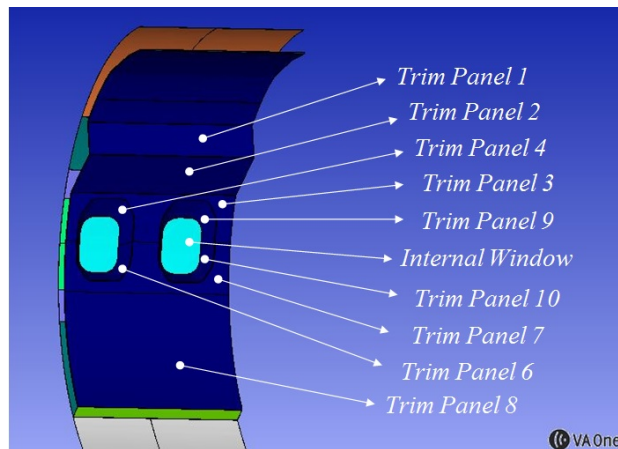


Figure 25: Internal nomenclature of the SEA panels

[t]0.48

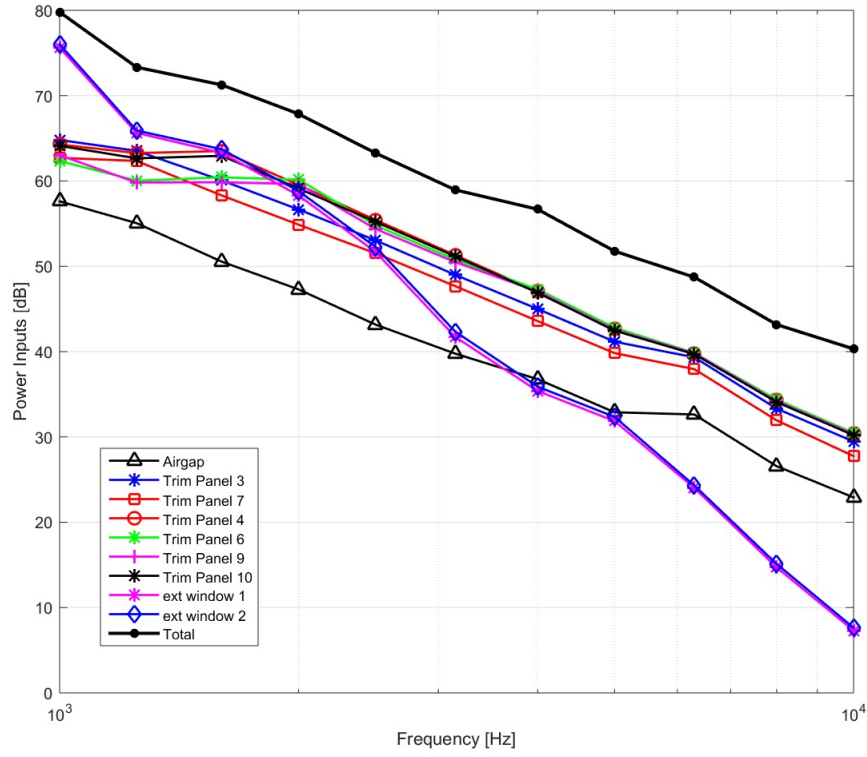


Figure 26: Power Inputs. Configuration B

[t]0.48

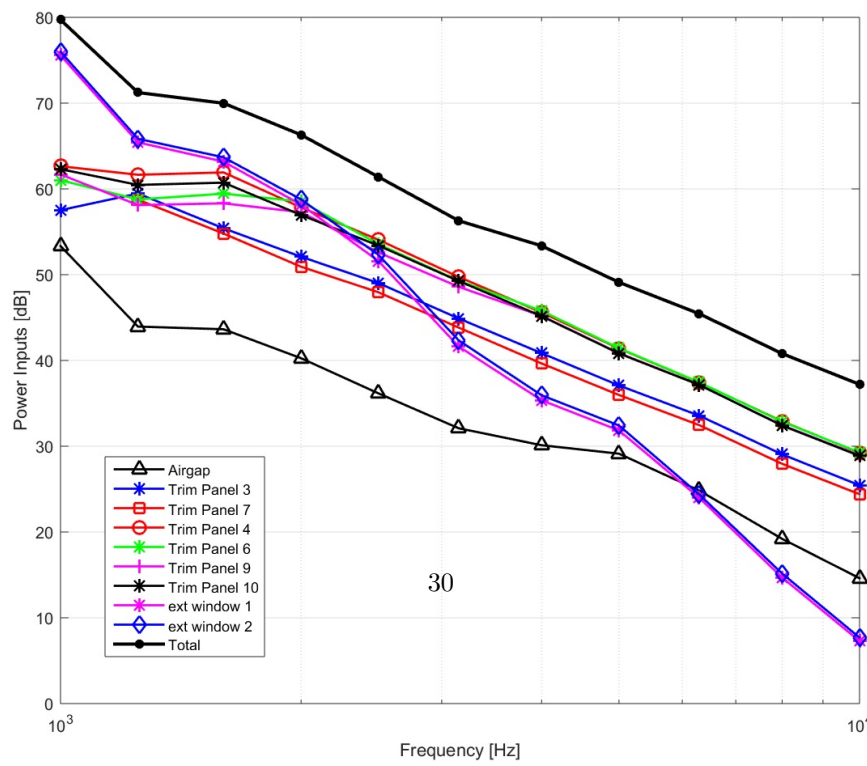


Figure 27: Power Inputs. Configuration C

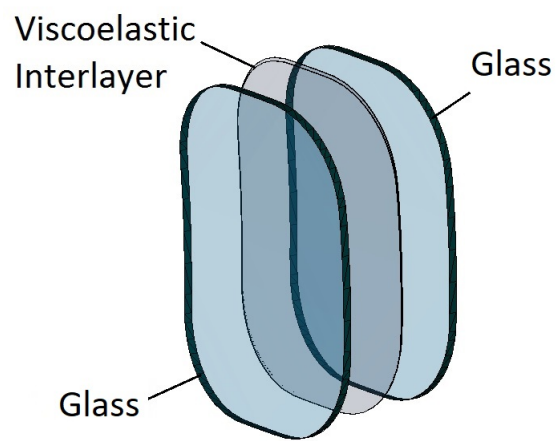
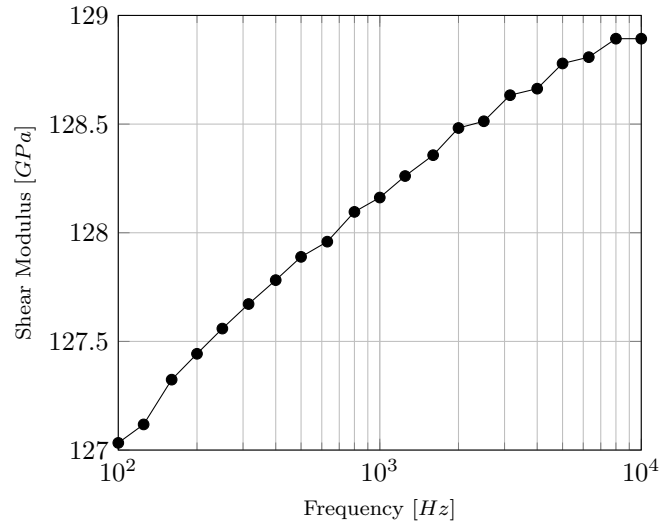
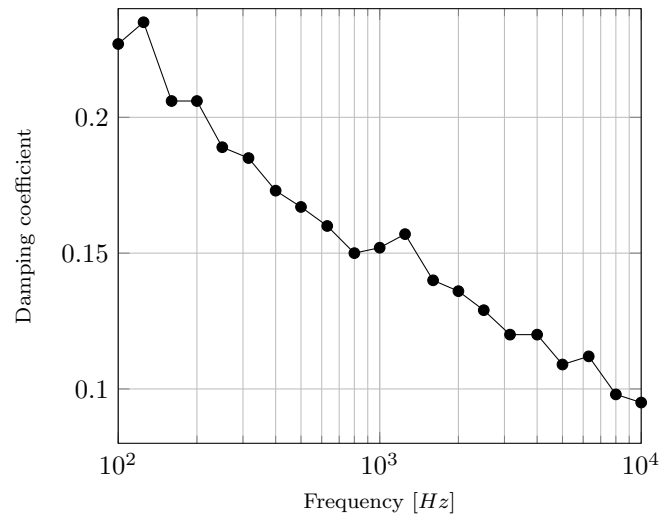


Figure 31: Viscoelastic interlayer sandwiched between two tempered glass layers



[t]0.48

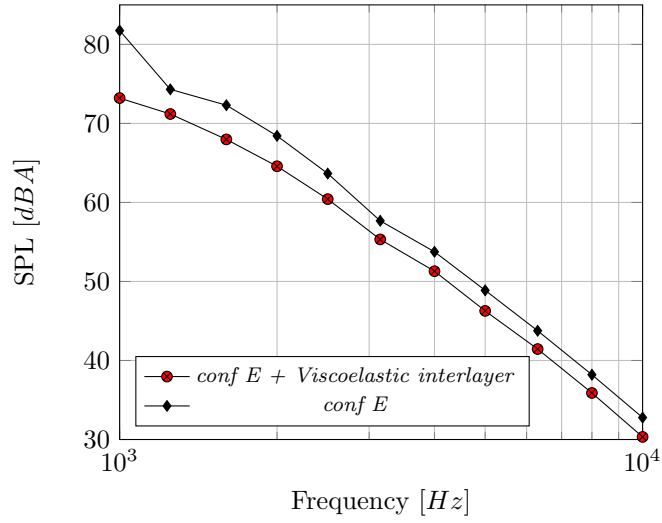
Figure 32: Solutia Saflex shear modulus [GPa]



[t]0.48

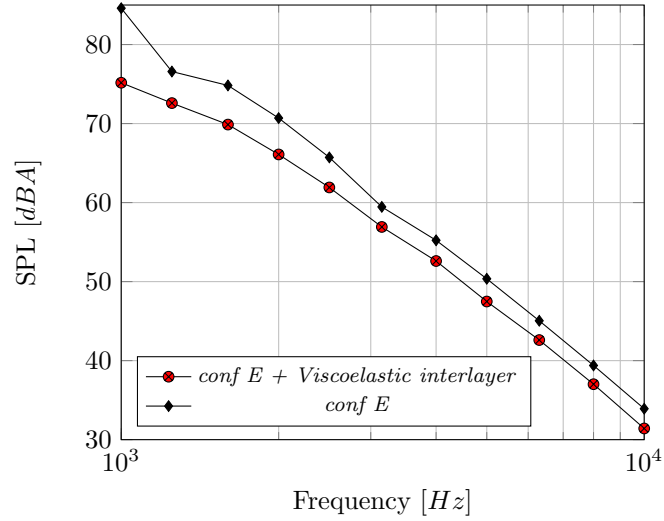
Figure 33: Solutia Saflex damping coefficient

Figure 34: Solutia Saflex mechanical properties: damping coefficient and shear modulus [dBA] in the range of frequency 100-10000 Hz



[t]0.48

Figure 35: Head cavity: Sec. III - three-seat layout side



[t]0.48

Figure 36: Head cavity: Sec. III - two-seat layout side

Figure 37: SPL over the Head cavities. Comparison between the *Configuration E* and the *Configuration E + Viscoelastic interlayer*. Range of frequency 1000-10000 Hz

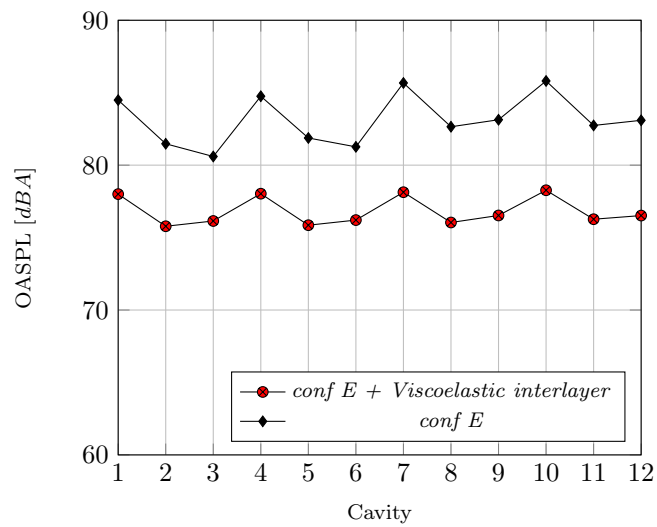


Figure 38: OASPL over the cavities present in the fuselage section. Comparison between the *Configuration E* and the *Configuration E + Viscoelastic interlayer*